

# Lipid metabolome-wide effects of the PPAR $\gamma$ agonist rosiglitazone<sup>S</sup>

Steven M. Watkins,<sup>1,\*</sup> Peter R. Reifsnnyder,<sup>†</sup> Huei-ju Pan,<sup>†</sup> J. Bruce German,<sup>§</sup> and Edward H. Leiter<sup>†</sup>

Lipomics Technologies, Inc.,\* 2545 Boatman Ave., West Sacramento, CA 95691; The Jackson Laboratory,<sup>†</sup> 600 Main St., Bar Harbor, ME; and Department of Food Science & Technology,<sup>§</sup> University of California, Davis, CA

**Abstract** Successful therapy for chronic diseases must normalize a targeted aspect of metabolism without disrupting the regulation of other metabolic pathways essential for maintaining health. Use of a limited number of single molecule surrogates for disease, or biomarkers, to monitor the efficacy of a therapy may fail to predict undesirable side effects. In this study, a comprehensive metabolomic assessment of lipid metabolites was employed to determine the specific effects of the peroxisome proliferator-activated receptor  $\gamma$  (PPAR $\gamma$ ) agonist rosiglitazone on structural lipid metabolism in a new mouse model of Type 2 diabetes. Dietary supplementation with rosiglitazone (200 mg/kg diet) suppressed Type 2 diabetes in obese (NZO  $\times$  NON)F1 male mice, but chronic treatment markedly exacerbated hepatic steatosis. The metabolomic data revealed that rosiglitazone *i*) induced hypolipidemia (by dysregulating liver-plasma lipid exchange), *ii*) induced de novo fatty acid synthesis, *iii*) decreased the biosynthesis of lipids within the peroxisome, *iv*) substantially altered free fatty acid and cardioliipin metabolism in heart, and *v*) elicited an unusual accumulation of polyunsaturated fatty acids within adipose tissue. These observations suggest that the phenotypes induced by rosiglitazone are mediated by multiple tissue-specific metabolic variables. **Key words:** Because many of the effects of rosiglitazone on tissue metabolism were reflected in the plasma lipid metabolome, metabolomics has excellent potential for developing clinical assessments of metabolic response to drug therapy.—Watkins, S. M., P. R. Reifsnnyder, H.-j. Pan, J. B. German, and E. H. Leiter. Lipid metabolome-wide effects of the PPAR $\gamma$  agonist rosiglitazone. *J. Lipid Res.* 2002. 43: 1809–1817.

**Supplementary key words** diabetes • lipid metabolism • metabolomics • steatosis • peroxisome proliferator-activated receptor  $\gamma$  • mouse

Subtle, but chronic, dysregulations of metabolism are the basis for many diseases of affluent societies. This is particularly true for diseases such as obesity, Type 2 diabetes,

and atherosclerosis. Successful intervention in these diseases with drugs or nutrition requires normalizing the targeted metabolism without producing defects in other metabolic pathways. Failure to do so may exchange a naturally developing pathology with a new one induced by the treatment. Therefore, accurate assessments of therapeutic effectiveness and safety must measure metabolism comprehensively, a goal that is impossible using single-biomarker analyses. Quantitative and comprehensive analyses of the metabolome can assess metabolic response to a therapy with much greater accuracy and power than biomarker approaches. In this study, a quantitative and comprehensive analysis of the structural lipid metabolome was applied to gain an understanding of the effects that the Type 2 diabetes drug rosiglitazone has on liver metabolism.

Thiazolidinediones (TZDs) are potent therapeutic agents that have proven successful in the treatment of Type 2 diabetes in rodent models and in humans (1). These compounds, including troglitazone, rosiglitazone, and pioglitazone, are believed to exert their benefit as high affinity agonists of peroxisome proliferator-activated receptor  $\gamma$  (PPAR $\gamma$ ), whose subsequent activation of multiple nuclear genes reduces hyperlipidemia and hyperglycemia and improves insulin sensitivity (2). Included among the many actions of TZDs are shifts in systemic lipid profiles, with decreases in serum lipid concentrations. However, these actions of TZDs are accompanied by increased adipogenesis and lipid accumulation in tissues. A major question associated with these drugs and their mechanism of action is whether the benefits to circulating lipid concentrations can be disassociated from metabolic side effects, including hepatic lipid accumulation. Troglitazone- and rosiglitazone-associated hepatotoxicity (steatosis) was recently reported in KK-*A*<sup>1</sup> mice in the absence

Abbreviations: PPAR $\gamma$ , peroxisome proliferator-activated receptor  $\gamma$ ; TZD, thiazolidinedione.

<sup>1</sup> To whom correspondence should be addressed.

e-mail: steve.watkins@lipomics.com

<sup>S</sup>The online version of this article (available at <http://www.jlr.org>) contains an additional 4 tables.

Manuscript received 19 April 2002 and in revised form 26 July 2002.  
Published, JLR Papers in Press, August 16, 2002.  
DOI 10.1194/jlr.M200169JLR200

Copyright © 2002 by Lipid Research, Inc.

This article is available online at <http://www.jlr.org>

Journal of Lipid Research Volume 43, 2002 1809

of increased hepatic triacylglycerides concentrations (3). In addition, a small number of human patients treated with troglitazone developed severe hepatotoxicity (4). Assessing the variable metabolic response to TZDs is therefore necessary to evaluate the safety or efficacy of TZDs in individuals.

In mice, diabetes genes are defined as obesity-predisposing genes capable of interacting deleteriously with other susceptibility loci, as well as with environmental factors, to elicit a state of impaired glucose tolerance and insulin resistance sufficiently severe to precipitate development of Type 2 diabetes (5, 6). A new mouse diabetes model that potentially reflects the more common polygenic forms of Type 2 diabetes prevalent in humans is the F1 male generated by crossing mice from the New Zealand Obese (NZO/HILt) and Nonobese Nondiabetic (NON/Lt) strains. F1 males of these two mouse strains develop early-onset obesity leading to a progressively more severe hyperinsulinemia and development of maturity-onset hyperglycemia in 90–100% of the males maintained on a standard rodent chow containing only 6% fat (5). Because preliminary studies showed that chronic feeding of troglitazone (2 g/kg diet) produced marked hepatic steatosis in these animals, they may provide an appropriate model for testing the potentially deleterious effects of TZD treatment on liver metabolism. These preliminary studies showed that rosiglitazone was a more potent anti-diabetic TZD than troglitazone. In this study, an assessment of the lipid metabolome (the concentration of each lipid class and each of its constituent fatty acids) was applied to evaluate the effect of chronic feeding of a low dose (0.2 g/kg diet) of rosiglitazone on the lipid metabolism of diabetic F1 males. Analysis of the results of the study revealed key targets of the actions of rosiglitazone, and putatively PPAR $\gamma$ , on lipid metabolism.

## MATERIALS AND METHODS

### Mice

(NZO  $\times$  NON)F1 male mice were bred and maintained as described previously (6). Thirteen obese and diabetic (NZO  $\times$  NON)F1 males between 29 and 33 weeks of age were split into two groups. A group of six males was fed (ad libitum) the maintenance (control) diet (NIH-31 containing 6% fat; Purina, Richmond, IN). Seven males were fed the same diet supplemented with 200 mg rosiglitazone/kg diet. Both diets were received in powdered form, pelleted, and irradiated by Research Diets, New Brunswick, NJ. After 4 weeks of feeding, the mice were euthanized by CO<sub>2</sub> inhalation, and blood was collected by heart puncture using a heparinized 25-gauge needle and syringe (5% heparin). Heart, liver, and inguinal adipose were collected, weighed, and frozen in liquid nitrogen for subsequent analysis. A section of each liver was used for histologic analysis (fixation in Telly's fluid and periodic acid-Schiff staining). Quantitative lipid metabolome analysis and RT-PCR (described below) were performed on frozen samples from control and rosiglitazone-treated mice.

### Phenotypes

Body weight was measured immediately pre-treatment and at 2 and 4 weeks during dietary treatment. Plasma glucose concen-

trations were measured immediately pre-treatment and after 4 weeks of treatment (Beckman Glucose 2 analyzer, Beckman Instruments, Fullerton, CA). Plasma insulin and leptin concentrations were measured at termination by rat insulin or mouse leptin radioimmuno assay kits (Linco, St. Charles, MO). A Synchron 5 chemistry analyzer (Beckman Instruments) was used for clinical chemistry. Plasma alanine aminotransferase was assessed as an indicator of liver damage. Total serum cholesterol and triacylglycerides were also measured.

### Gene expression

Total RNA was isolated from slices of frozen livers and inguinal adipose tissue from five mice per group using Trizol and following the protocol supplied by the manufacturer (Gibco-BRL, Gaithersburg, MD). Details regarding cDNA preparation, primer pair sequences for the transcripts shown in Table 2 and 3, and the conditions used for specific gene amplification in an ABI Prism<sup>®</sup> 7700 Sequence Detection System (PE Applied Biosystems, Foster City, CA) can be found at <http://www.jax.org/research/leiter/documents/databases.html>.

Gene expression data were obtained by measuring the fluorescence intensity for each PCR reaction using the system software and was analyzed in Excel<sup>®</sup> (Microsoft Corporation, Redmond, WA).  $C_T$  is the PCR cycle number where amplification shifts from linear to logarithmic.  $\Delta C_T$  is the difference between the target gene and the internal reference (18S RNA).  $\Delta\Delta C_T$  is the difference for the  $\Delta C_T$  for the target gene as a function of treatment. Fold-differences are expressed as  $2^{-\Delta\Delta C_T}$ .

### Lipid metabolome data

The lipids from plasma and tissues were extracted in the presence of authentic internal standards by the method of Folch et al. (7) using chloroform-methanol (2:1, v/v). Heart or liver tissue (25 mg), 200  $\mu$ l plasma, or 10 mg inguinal adipose tissue was used for each analysis. Individual lipid classes within each extract were separated by preparative thin-layer chromatography as described previously (8). Authentic lipid class standard compounds were spotted on the two outside lanes of the thin-layer chromatography plate to enable localization of the sample lipid classes. Each lipid fraction was scraped from the plate and trans-esterified in 3 N methanolic-HCl in a sealed vial under a nitrogen atmosphere at 100°C for 45 min. The resulting fatty acid methyl esters were extracted from the mixture with hexane containing 0.05% butylated hydroxytoluene and prepared for gas chromatography by sealing the hexane extracts under nitrogen.

Fatty acid methyl esters were separated and quantified by capillary gas chromatography using a gas chromatograph (Hewlett-Packard model 6890, Wilmington, DE) equipped with a 30 m DB-225MS capillary column (J&W Scientific, Folsom, CA) and a flame-ionization detector as described previously (8).

### Data processing and statistics

Significance of differences in phenotypic parameters between rosiglitazone treated and control mice as well as treatment effects on tissue lipid metabolite concentrations were assessed by unpaired Student's *t*-tests, with significance assumed at  $P \leq 0.05$ . For the quantitative PCR comparisons of transcript levels in liver and inguinal fat, a paired Student's *t*-test assuming unequal variance was performed and a Bonferroni correction was made for multiple comparisons ( $\alpha$ , 0.0042).

Quantitative (nmol/g) data were visualized using the Lipomics Surveyor<sup>™</sup> software system, which creates a "heat-map" graph of the difference between the data for treated and control mice. The Surveyor<sup>™</sup> data (see Results) are read as follows: the column headers display the fatty acid and the family of fatty acids present in each lipid class, which are in turn described in the row

headers. The lipid classes are grouped by tissue. The heat map displays an increase in each metabolite in rosiglitazone-treated mice relative to control mice as a green square and a decrease in a metabolite as a red square. The brightness of the square indicates the magnitude of the difference, as detailed in the figure legends.

## RESULTS

### Phenotypic assessment of rosiglitazone treatment

Prior to dietary treatment with rosiglitazone, both the treated group and the control group of mice were comparably obese and chronically diabetic. The pre-treatment mean plasma glucose concentrations and body weights for the rosiglitazone-treated group were not significantly different from the untreated group (Table 1). After 4 weeks of rosiglitazone treatment, diabetic hyperglycemia was completely reversed, and the reversal of hyperglycemia was accompanied by significant declines in plasma concentrations of insulin, leptin, triacylglycerides, and cholesterol (Table 1). Despite the decrease in plasma lipids with treatment, mice treated with rosiglitazone gained significantly more body weight than control mice (Table 1), and this treated group exhibited significantly increased mean wet weights in inguinal (but not gonadal) fat, heart, liver, and pancreas (data not shown). Increased serum alanine aminotransferase in treated mice compared with control mice indicated rosiglitazone-associated hepatotoxicity. Figure 1 shows liver histopathology for both groups. Whereas both groups of mice showed multiple foci of macrovesicular fat accumulation, hepatic lipidosis, as evidenced by macrovesicular fat droplets within hepatocytes, was greater in rosiglitazone-treated mice (Fig. 1B) than in control mice (Fig. 1A).

### Quantitative gene expression

Quantitative gene expression data were collected for selected genes involved in lipid metabolism. In liver, quantitative differences in expression of genes encoding adiponectin (ADN), fatty acid binding protein 4 (commonly called aP2), fatty acid synthase (FAS), lipoprotein lipase (LPL), fatty acid translocase (CD36), peroxisome proliferator-activated receptors (PPAR $\alpha$ , PPAR $\gamma$ 1, and PPAR $\gamma$ 2), acetyl-

CoA carboxylase (ACC), acetyl-CoA oxidase (ACO), cytochrome P450 4A1 (CYP4a1), and carnitine palmitoyl transferase 1 $\alpha$  (CPT1a) between treated and untreated mice were determined as described in the Materials and Methods. In confirmation of the morphology showing increased lipid accumulation in livers of rosiglitazone treated males, ADN, aP2, FAS, and LPL transcripts were quantitatively greater in treated mice relative to untreated controls (Table 2). The expression of PPAR $\gamma$ 1, PPAR $\gamma$ 2, and PPAR $\alpha$  did not differ significantly between the groups (Table 2). The greater expression of FAS is consistent with the greater concentrations of 16:1n7 and 18:1n7 observed in treated mice relative to untreated mice, and together these observations demonstrate a clear upregulation of de novo fatty acid synthesis with rosiglitazone treatment. Increases in ADN and aP2 transcripts, both associated with adipogenesis, are consistent with the lipid metabolome profiles showing rosiglitazone-induced increases in hepatic lipid accumulation.

Table 3 shows rosiglitazone-mediated differences in gene expression in inguinal fat. In addition to the transcript panel described in Table 2, additional adipocyte-expressed transcripts analyzed included those of the family of uncoupling proteins (UCP1, UCP2, and UCP3), leptin, and tumor necrosis factor  $\alpha$  (TNF $\alpha$ ). The most striking difference was a 192-fold upregulation of UCP1 transcription. Adipsin, a marker of adipogenesis, was significantly decreased. A rosiglitazone-induced 6.7-fold increase in FAS, although not statistically significant after correction for multiple comparisons, correlated with the observed increase in UCP1 as well as the lipid metabolome profile showing increased 16:1n7 and 18:1n7 concentrations in inguinal adipose tissue (Fig. 2).

### Metabolomic assessment of plasma lipids

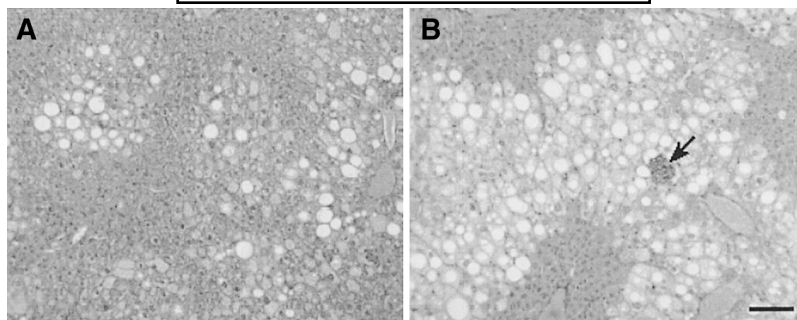
The results of the quantitative assessment of the plasma lipid metabolome in rosiglitazone-treated and untreated mice are shown in Table 4 of the Supplemental Data and in Fig. 2 and Fig. 3. Lipid metabolite concentrations in plasma confirmed the rosiglitazone-induced depletion of specific classes of plasma lipids. Significant rosiglitazone-mediated decreases in phosphatidylcholine, triacylglyceride, and cholesterol ester distinguished rosiglitazone-treated mice from untreated mice, whereas no significant decreases in sphingomyelin, phosphatidylethanolamine, or free fatty acids were observed (Fig. 2). Phosphatidylcholine and triacylglycerides are derived principally from liver lipid export. Total plasma triacylglyceride concentrations were lower in treated mice (400 nmol/g) than in untreated mice (1,400 nmol/g) (Fig. 2). The concentrations of total plasma free fatty acids, which are derived principally from adipose tissue, were not affected by rosiglitazone treatment. Although the total concentrations of phosphatidylcholine and cholesterol ester were lower in rosiglitazone-treated mice than in untreated mice, the absolute concentration of palmitoleic acid (16:1n7) within these lipid classes and within free fatty acids was higher in treated mice than in controls (Fig. 3). The increased palmitoleic acid concentrations in plasma were reflective

TABLE 1. Phenotypic changes<sup>a</sup> following 4-week rosiglitazone treatment

Phenotype	Control	Rosiglitazone	P <sup>b</sup>
Body weight (g)-start	66.6 ± 1.3	67.3 ± 1.3	NS
Body weight (g)-end	70.6 ± 1.5	81.6 ± 1.0	<0.001
Plasma glucose (mg/dl)-start	387 ± 41	350 ± 31	NS
Plasma glucose (mg/dl)-end	446 ± 22	160 ± 13	<0.001
Plasma insulin (ng/ml)	65.0 ± 5.5	4.1 ± 0.4	<0.001
Plasma leptin (ng/ml)	54.6 ± 5.5	42.4 ± 1.6	0.043
Plasma cholesterol (mg/dl)	190 ± 12	124 ± 5	<0.001
Plasma triacylglycerides (mg/dl)	145 ± 13	56 ± 9	<0.001
Plasma alanine aminotransferase (IU/l)	60 ± 14.5	100 ± 6.1	0.021

<sup>a</sup> Data are means and SEM for each group.

<sup>b</sup> Test of significant main effect of treatment by ANOVA.



**Fig. 1.** Severe hepatic steatosis following 4 weeks of rosiglitazone treatment. A: Liver of control diet-fed mouse shows foci of macrovesicular lipidosis in hepatocytes. B: Liver of a rosiglitazone-treated male mouse shows massive lipidosis with displacement of hepatic parenchyma. Arrow denotes focus of inflammatory cells, including neutrophils. Sections stained with Periodic-acid Schiff (PAS) for glycogen. Bar denotes 100  $\mu\text{m}$ .

of the increased de novo lipogenesis occurring within the liver and adipose tissue (see below).

### Liver lipid metabolism

The results of the quantitative assessment of the liver lipid metabolome in rosiglitazone-treated and untreated mice are shown in Table 5 of the Supplemental Data and in Figs. 2 and 3. Lipid metabolites in the liver demonstrated a reciprocal relation between liver and plasma lipid concentrations. The significant rosiglitazone-mediated decreases in plasma triacylglycerides were balanced by a substantial accumulation of triacylglycerides within the liver (Figs. 2, 3). Total hepatic triacylglycerides were 81,300 nmol/g in untreated mice and 150,400 nmol/g in the rosiglitazone-treated mice. The concentrations of other lipid classes were not affected by rosiglitazone treatment with the exception of sphingomyelin, which was present at 1,180 nmol/g in treated mice and at 1,890 nmol/g in untreated control mice (Fig. 2). This rosiglitazone-induced

reciprocity between liver and plasma triacylglycerides is consistent with an inhibition of normal liver-plasma lipid exchange. No change was observed in the total concentration of phosphatidylcholine or cholesterol ester in liver as a consequence of rosiglitazone treatment (Fig. 2).

### Heart lipid class metabolism

The results of the quantitative assessment of the heart lipid metabolome in rosiglitazone-treated and untreated mice are shown in Table 6 of the Supplemental Data and in Figs. 2 and 3. Free fatty acids are the primary source of energy for the heart. The average concentration of total free fatty acid in the heart was 5,100 nmol/gm untreated mice and 2,500 nmol/g in rosiglitazone-treated mice (Fig. 2). This difference was largely independent of the type of free fatty acid, as the saturated n-3, n-6, and n-9 families of fatty acids were all approximately 50% lower in treated mice than in untreated mice (Fig. 2). The free n-7 fatty acids were not depleted as substantially from heart, likely due to the increased biosynthesis of n-7 fatty acids and corresponding increased concentration of n-7 fatty acids within the triacylglycerides and free fatty acids of plasma.

TABLE 2. Quantitative changes in hepatic gene transcript levels induced by rosiglitazone feeding<sup>a</sup>

Gene Products	$\Delta\Delta C_T$ (Rosi-Control)	Fold Change $2^{-\Delta\Delta C_T}$	P Value
Adipsin (ADN)	-6.56	94.66	0.0002
Fatty acid binding protein 4 (aP2)	-4.91	30.06	0.0002
Fatty acid synthase (FAS)	-2.60	6.06	0.0001
Lipoprotein lipase (LPL)	-2.51	5.71	0.004
Fatty acid translocase (CD36)	-1.13	2.19	0.12
Peroxisome proliferator-activated receptor $\gamma$ 1 (PPAR $\gamma$ 1)	0.03	0.97	0.97
Peroxisome proliferator-activated receptor $\gamma$ 2 (PPAR $\gamma$ 2)	-0.04	1.03	0.96
Acetyl-CoA carboxylase (ACC)	0.07	0.95	0.90
Peroxisome proliferator-activated receptor $\alpha$ (PPAR $\alpha$ )	0.51	0.70	0.08
Acetyl-CoA oxidase (ACO)	-1.03	2.04	0.15
Cytochrome P450 4A1 (CYP4A1)	-0.94	1.92	0.14
Carnitine palmitoyl transferase 1 $\alpha$ (CPT1 $\alpha$ )	0.37	0.77	0.55

Statistical significance between the two groups was determined using a paired Student's *t*-test assuming unequal variances and correcting for multiple comparisons ( $\alpha$ , 0.0042).

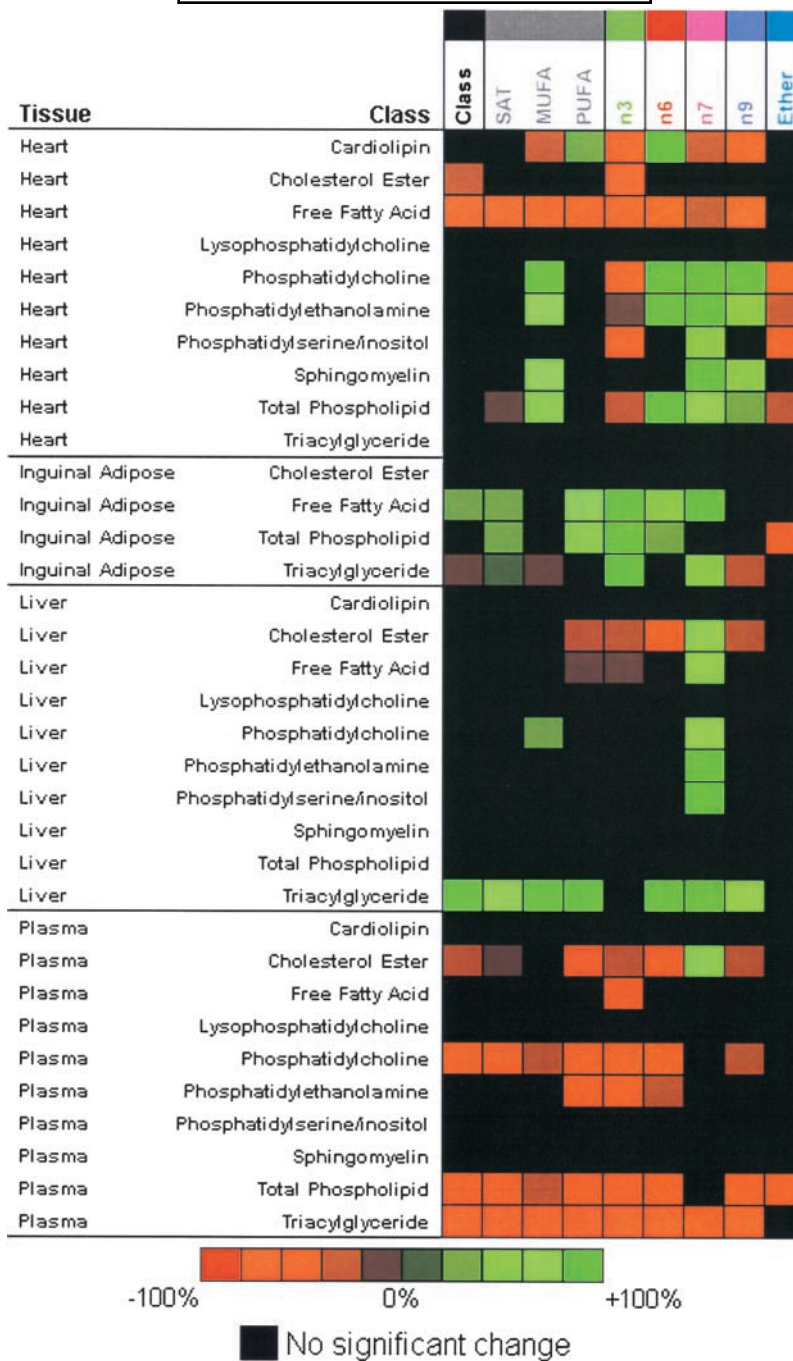
<sup>a</sup> Quantitative (real-time) PCR was performed on hepatic RNA extracted from five individual mice per group as described in Materials and Methods.

TABLE 3. Quantitative changes in inguinal fat gene transcript levels induced by rosiglitazone feeding<sup>a</sup>

Gene Products	$\Delta\Delta C_T$ (Rosi-Control)	Fold Change $2^{-\Delta\Delta C_T}$	P Value
Uncoupling protein 1 (UCP1)	-7.59	192.97	0.00095
Fatty acid synthase (FAS)	-2.74	6.69	0.036
Adipsin (ADN)	2.86	0.14	0.0042
Leptin	1.45	0.37	0.046
Tumor necrosis factor $\alpha$ (TNF $\alpha$ )	2.68	0.16	0.0047
Uncoupling protein 2 (UCP2)	1.71	0.30	0.013
Acetyl-CoA oxidase (ACO)	-1.02	2.03	0.12
Acetyl-CoA carboxylase (ACC)	-0.66	1.58	0.22
Fatty acid binding protein 4 (aP2)	-0.25	1.19	0.61
Uncoupling protein 3 (UCP3)	0.76	0.59	0.29
PPAR $\gamma$ 1	0.27	0.83	0.52
PPAR $\gamma$ 2	0.94	0.52	0.54

Statistical significance between the two groups was determined using a paired Student's *t*-test and correcting for multiple comparisons ( $\alpha$ , 0.0042).

<sup>a</sup> Quantitative (real-time) PCR was performed on inguinal fat RNA extracted from five individual mice per group as described in Materials and Methods.



**Fig. 2.** Rosiglitazone treatment exerts strong and tissue-specific effects on lipid class metabolism. The concentration (expressed in nmol/g sample) of each lipid metabolite from treated and untreated mice was used to generate the summary data displayed here as a heat map. The first column displays the quantitative difference in the concentration of each lipid class between the groups. The next columns, in order, describe the quantitative difference in the concentration of saturated fatty acids, monounsaturated fatty acids, polyunsaturated fatty acids, n3 fatty acids, n6 fatty acids, n7 fatty acids, n9 fatty acids, and plasmalogen lipids among the groups. The magnitude of the difference, expressed as a percentage change in the quantitative data between treated and untreated mice, is represented by color according to the legend. Differences not meeting a  $P < 0.05$  are displayed in black.

The hearts of rosiglitazone-treated mice were significantly enriched with cardiolipin, the primary structural lipid of the inner mitochondrial membrane. The mean cardiolipin content of hearts from rosiglitazone-treated mice was 3,000 nmol/g as compared with 2,500 nmol/g in

untreated mice. Unlike free fatty acids, the fatty acid components of cardiolipin were differentially modulated by rosiglitazone treatment. The primary fatty acid of cardiolipin, linoleic acid (18:2n6), was 4,550 nmol/g in control heart cardiolipin and 8,850 nmol/g in heart cardiolipin of

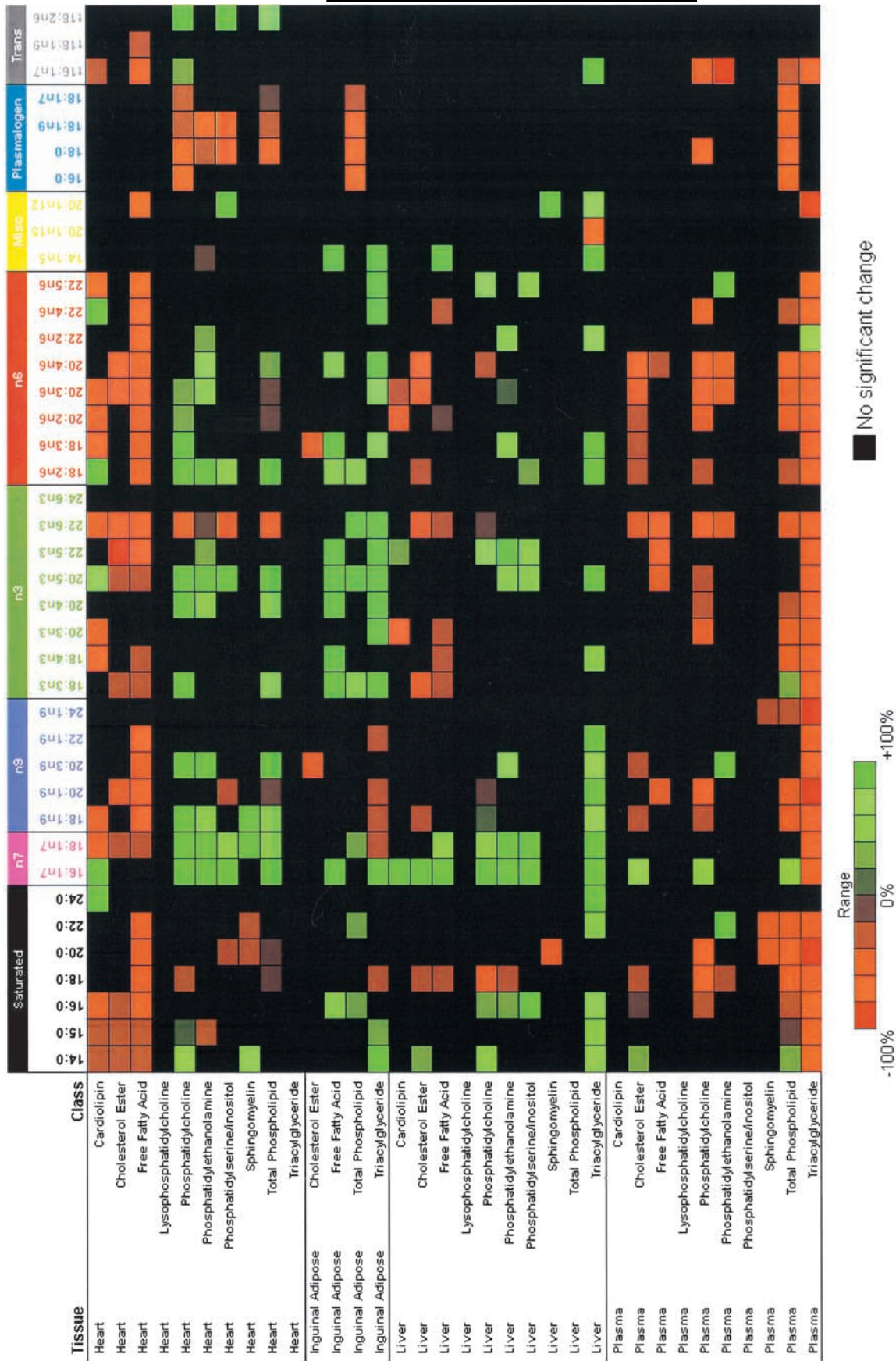


Fig. 3. The effect of rosiglitazone treatment on individual lipid metabolites. The concentration (expressed in nmol/g sample) of each lipid metabolite from treated and untreated mice was used to generate a heat map. The column headers represent an individual fatty acid present in the lipid classes displayed on the left. The magnitude of the difference, expressed as a percentage change in the quantitative data between treated and untreated mice, is represented by color according to the legend. Differences not meeting a  $P < 0.05$  are displayed in black.

rosiglitazone-treated mice. Docosahexaenoic acid (22:6n3) was depleted from cardiolipin in the hearts of treated mice (950 nmol/g) relative to hearts of control mice (2,200 nmol/g).

The plasmalogen lipids, those lipids that contain 1-enyl-ether-linked alkyl chains, are derived from the dihydroxyacetone phosphate pathway and are partially synthesized within the peroxisome (9). The concentration of plasmalogens was lower in the heart phospholipids of mice treated with rosiglitazone than of controls (Fig. 3). These data are consistent with a decreased peroxisomal synthesis of lipids within the hearts of treated mice.

#### Adipose lipid class metabolism

The results of the quantitative assessment of the inguinal adipose lipid metabolome in rosiglitazone-treated and untreated mice are shown in Table 7 of the Supplemental Data and in Figs. 2 and 3. Inguinal fat tissue from rosiglitazone-treated mice displayed a 5.7% lower triacylglyceride content (9,628  $\mu\text{mol/g}$ ) than inguinal adipose from controls (1,019  $\mu\text{mol/g}$ ), and 35% more free fatty acids (13,370 nmol/g in treated mice and 9,900 nmol/g in controls). No significant differences in total phospholipid or cholesterol ester concentrations were observed (Fig. 2).

The fatty acid composition of inguinal fat triacylglycerides was substantially altered by rosiglitazone treatment, with inguinal fat from treated mice accumulating fatty acids from the saturated, n-7, and n-3 families of fatty acids while being depleted of the n-9 family of fatty acids (Fig. 2). In particular, an unusual accumulation of n-3 fatty acids was observed in inguinal fat from rosiglitazone-treated animals. The concentration of total n-3 fatty acids in the inguinal fat triacylglycerides of treated mice was 71,260 nmol/g, representing a 120% greater concentration than that in untreated mice (Fig. 2). The most notable increases within the n-3 family of fatty acids were a 522% greater concentration (4,100 nmol/g) of eicosapentaenoic acid, a 612% greater concentration (7,000 nmol/g) of docosahexaenoic acid, and 84% (24,300 nmol/g) more  $\alpha$ -linolenic acid in inguinal fat triacylglycerides in treated as compared with control mice (Fig. 3). The concentration of n-7 fatty acids in inguinal fat triacylglycerides was 303  $\mu\text{mol/g}$  in treated mice and 204  $\mu\text{mol/g}$  in untreated controls (Fig. 2). In contrast, the total concentration of n-6 fatty acids was less than 3% higher. However, the accumulation or depletion of individual fatty acids within the n-6 family varied substantially. Whereas linoleic acid (18:2n6), by far the most prominent n-6 fatty acid in inguinal fat, was not significantly altered by treatment, the concentrations of  $\gamma$ -linolenic, dihomogamma-linolenic, and arachidonic acids in inguinal fat were respectively, 1,225 nmol/g (78%), 1,300 nmol/g (64%), and 3,800 nmol/g (276%) greater in treated mice than in untreated controls (Fig. 3).

The concentration of plasmalogen lipids in inguinal fat phospholipids was depleted by rosiglitazone treatment (Fig. 2). The concentration of total plasmalogen fatty acids from the phospholipids of inguinal fat was 130 nmol/g (60%) less in treated mice than untreated controls.

## DISCUSSION

Rosiglitazone treatment is often accompanied by weight gain in humans (10), an effect strikingly reflected by the rosiglitazone-induced increase in body weight of already markedly-obese (NZO  $\times$  NON)F1 male mice. In this study, the potent anti-hyperglycemic effect of rosiglitazone was accompanied by an increased de novo synthesis of fatty acids. This result obtained by lipid metabolome profiling corroborated gene expression analysis of liver and inguinal fat, wherein both tissues showed upregulated expression of genes associated with adipogenesis and fatty acid synthesis. A recent gene expression profiling of livers of C57BL6J ICAM-1 deficient mice fed a high-fat diet also showed upregulated adipin expression concomitant with fatty liver development (11). Interestingly, in inguinal fat, wherein expression of the gene encoding UCP1 was markedly upregulated by rosiglitazone treatment, expression of the adipin gene was significantly reduced. Palmitoleic acid (16:1n7) and vaccenic acid (18:1n7) were excellent metabolic indicators of the increased de novo synthesis of fatty acids in both liver and adipose, an effect that corresponded with an increased expression of fatty acid synthase. This increased synthesis of fatty acids was likely a key metabolic explanation for both the hepatic weight gain and the severe hepatic steatosis observed in the rosiglitazone-treated animals. Interestingly, although lipid biosynthesis was increased, the increase in liver triacylglyceride concentration was not reflected in the plasma. Thus, there was a strong indication that normal lipid import-export activities between the liver and plasma were impaired by rosiglitazone treatment, and that this dysregulation and increased biosynthesis of lipids was mutually responsible for the hepatic steatosis. In previous studies describing short TZD treatments in obese-diabetic rodent models, troglitazone was not reported to produce hepatotoxicity (12, 13). TZD-treated leptin-deficient C57BL/6J-*Lep<sup>ob</sup>/Lep<sup>ob</sup>* ("obese") mice, ZDF-*Lep<sup>fa</sup>/Lep<sup>fa</sup>* ("fatty") rats, or mice genetically-engineered to have reduced white or brown adipose depots were also not found to exhibit significant increases in hepatic triacylglyceride concentrations, nor was hepatotoxicity reported (14, 15). However, troglitazone- and rosiglitazone-associated hepatotoxicity (steatosis) was recently reported in KK-*A*<sup>y</sup> mice in the absence of increased hepatic triacylglyceride levels (3). Thus, published studies of obese-diabetic mice on different inbred strain backgrounds show considerable differences in hepatic responses to TZD treatment. However, none of the published studies reported hepatic accumulation of both triacylglycerides and cholesterol esters to the extent we observed in (NZO  $\times$  NON)F1 males. Hence, (NZO  $\times$  NON)F1 males may exhibit underlying defects in lipid metabolism not present in the other genetic models and these strain-specific metabolic defects may render them particularly prone to TZD-induced steatosis.

Because rosiglitazone decreased the concentrations of plasma lipids as classes of molecules (i.e., triacylglycerides, cholesterol esters, etc.), standard clinical markers of lipid metabolism (Table 1) did not reflect the increased he-


patic de novo lipogenesis in response to rosiglitazone treatment. In contrast, the metabolomic assessment of plasma lipids identified several markers of increased liver lipogenesis, including an increased absolute concentration of 16:1n7 and 18:1n7 in plasma cholesteryl esters, phosphatidylcholine, and triacylglycerides, despite the decrease in the concentration of total plasma lipid classes. The metabolomic analysis of the plasma alone was therefore capable of making the important discrimination between hypolipidemia caused by decreased lipid synthesis compared with hypolipidemia caused by impaired export of lipid by the liver. These data suggest that metabolomic analyses of human plasma may have strong potential as clinical diagnostics. Further demonstrating the strong relations between the plasma lipid metabolome and tissue metabolism were the decreased concentration of plasmalogen lipids in plasma and the similarity between the composition of the plasma lipid metabolome and liver and adipose metabolomes.

Heart lipid metabolism was strongly influenced by rosiglitazone treatment. In particular, heart free fatty acids, cardiolipin, plasmalogen lipids, and the important polyunsaturated fatty acids 22:6n3 and 18:2n6 were significantly modulated by treatment. Some of these changes, particularly those involving the concentration and composition of cardiolipin and free fatty acids, may in part represent the alterations in muscle metabolism that improve insulin sensitivity. Cardiolipin is an essential phospholipid for energy metabolism and the primary phospholipid of the inner mitochondrial membrane (16–18). The content and composition of cardiolipin are important to the efficiency of electron transport. Rosiglitazone caused an increase in heart cardiolipin concentration and a substantial remodeling of cardiolipin toward an elevated 18:2n6 content and a diminished 22:6n3 content. Interestingly, this is precisely the change in cardiolipin content and composition that would increase electron transport efficiency (17, 19–21) and decrease electron leakage (22), according to the existing *in vitro* data. Rosiglitazone-induced remission from hyperglycemia in combination with reduced plasma insulin concentrations indicated that glucose oxidation by tissues was increased by this insulin-sensitizing agent. Thus, it is possible that increased energy metabolism as well as decreased plasma lipids may have caused the decreased heart free fatty acid concentrations.

Two major types of lipids quantified in this study are synthesized at least in part within the peroxisome. These are the fatty acids with three double bonds on the carboxylic acid side of an n9 double bond (22:5n6 and 22:6n3) (23–25), and the plasmalogen lipids, which are synthesized by the dihydroxyacetone phosphate biosynthetic pathway (9). Heart tissue from rosiglitazone-treated mice contained significantly less 22:6n3 in phosphatidylcholine, phosphatidylethanolamine, cardiolipin, phosphatidylserine/inositol, free fatty acids, and cholesterol esters than did heart from untreated control mice. Additionally, there was a significant depletion of plasmalogen lipids from the heart phospholipids of treated mice relative to untreated controls. These observations suggest that rosi-

glitazone, a known PPAR $\gamma$  agonist, has an inhibitory effect on lipid biosynthesis in the peroxisome. The decreased production of 22:6n3 and plasmalogen lipid may have important physiologic consequences. Dietary 22:6n3 has well-documented positive effects on cardiac function (26–31), and plasmalogen lipids have recently been shown to be essential to membrane trafficking and the structure of caveolae, clathrin-coated pits, endoplasmic reticulum, and Golgi cisternae (32).

A curious finding in this study was the inguinal fat tissue accumulation of polyunsaturated fatty acids in response to rosiglitazone. The accumulation of 22:6n3 and other long-chain polyunsaturated fatty acids likely occurs via a pathway independent of their biosynthesis *de novo* from precursors. The conversion of polyunsaturated-rich phospholipids to triacylglycerides via a phospholipase C pathway also does not appear to be the primary metabolic basis for the enrichment with polyunsaturates, as phospholipids were also enriched with polyunsaturated fatty acids. This unusual response may be an important clue to understanding the physiology of adipose tissue activated by PPAR $\gamma$  agonists, and should be investigated further.

The present study utilized a diabetic mouse model in which the anti-diabetic action of a TZD was accompanied by excessive weight gain and major alterations in the lipid metabolome. Its major findings were that rosiglitazone *i*) induced hypolipidemia by disrupting the mobilization of liver lipids into plasma, *ii*) induced *de novo* fatty acid synthesis, *iii*) diminished the biosynthesis of lipid synthesized within the peroxisome, *iv*) had substantial effects on heart cardiolipin and free fatty acid metabolism, and *v*) exerted tissue-specific effects on lipid metabolism. The unusually high sensitivity of the diabetic (NZO  $\times$  NON)F1 male to thiazolidinedione-induced lipid accumulation in liver may be related to the observation that a moderate level of hepatic steatosis had already initiated in the diabetic control group fed a chow diet containing only 6% fat. We hypothesize that these F1 mice have underlying defects in hepatic lipid metabolism that render them particularly sensitive to the steatosis-inducing effects of TZDs. Elucidation of the metabolic and pharmacogenetic bases for the metabolic responses to rosiglitazone described in this study will be valuable in determining markers of efficacy and safety for TZD treatment in humans and for defining species and individual-specific responses to TZDs. However, it should be noted that lipid metabolism in mice is distinct in many ways from that in humans, and that the direct applicability of these data to human subjects remains to be tested. 

The physiogenomic work performed at The Jackson Laboratory was supported by National Institutes of Health Grant DK56853 (E.H.L.) and was approved by the institution's Animal Care and Use Committee. H.P. was supported by an American Diabetes Association postdoctoral fellowship. Institutional shared services (T.J.L.) were supported by National Cancer Institute Cancer Center Support Grant CA-34196. The authors thank Bruce Regimbal and C. J. Dillard for technical assistance.



## REFERENCES

1. Spiegelman, B. M. 1998. PPAR-gamma: adipogenic regulator and thiazolidinedione receptor. *Diabetes*. **47**: 507–514.
2. Saltiel, A. R., and J. M. Olefsky. 1996. Thiazolidinediones in the treatment of insulin resistance and type II diabetes. *Diabetes*. **45**: 1661–1669.
3. Bedoucha, M., E. Atzpodien, and U. A. Boelsterli. 2001. Diabetic KKAY mice exhibit increased hepatic PPARgamma1 gene expression and develop hepatic steatosis upon chronic treatment with antidiabetic thiazolidinediones. *J. Hepatol*. **35**: 17–23.
4. Parulkar, A. A., M. L. Pendergrass, R. Granda-Ayala, T. R. Lee, and V. A. Fonseca. 2001. Nonhypoglycemic effects of thiazolidinediones. *Ann. Intern. Med.* **134**: 61–71.
5. Leiter, E. H., P. C. Reifsnnyder, K. Flurkey, H. J. Partke, E. Junger, and L. Herberg. 1998. NIDDM genes in mice: deleterious synergism by both parental genomes contributes to diabetogenic thresholds. *Diabetes*. **47**: 1287–1295.
6. Reifsnnyder, P. C., G. Churchill, and E. H. Leiter. 2000. Maternal environment and genotype interact to establish diabetes in mice. *Genome Res.* **10**: 1568–1578.
7. Folch, J., M. Lees, and G. H. Sloane-Stanley. 1957. A simple method for the isolation and purification of total lipids from animal tissues. *J. Biol. Chem.* **226**: 497–509.
8. Watkins, S. M., T. Y. Lin, R. M. Davis, J. R. Ching, E. J. DePeters, G. M. Halpern, R. L. Walzem, and J. B. German. 2001. Unique phospholipid metabolism in mouse heart in response to dietary docosahexaenoic or  $\alpha$ -linolenic acids. *Lipids*. **36**: 247–254.
9. Nagan, N., and R. Zoeller. 2001. Plasmalogens: biosynthesis and functions. *Prog. Lipid Res.* **40**: 199–229.
10. Fuchtenbusch, M., E. Standl, and H. Schatz. 2000. Clinical efficacy of new thiazolidinediones and glinides in the treatment of type 2 diabetes mellitus. *Exp. Clin. Endocrinol. Diabetes*. **108**: 151–163.
11. Gregoire, F. M., Q. Zhang, S. J. Smith, C. Tong, D. Ross, H. Lopez, and D. B. West. 2002. Diet-induced obesity and hepatic gene expression alterations in C57BL/6J and ICAM-1-deficient mice. *Am. J. Physiol. Endocrinol. Metab.* **282**: E703–713.
12. Fujiwara, T., A. Okuno, S. Yoshioka, and H. Horikoshi. 1995. Suppression of hepatic gluconeogenesis in long-term Troglitazone treated diabetic KK and C57BL/KsJ-db/db mice. *Metabolism*. **44**: 486–490.
13. Shimabukuro, M., Y. T. Zhou, Y. Lee, and R. H. Unger. 1998. Troglitazone lowers islet fat and restores beta cell function of Zucker diabetic fatty rats. *J. Biol. Chem.* **273**: 3547–3550.
14. Memon, R. A., L. H. Tecott, K. Nonogaki, A. Beigneux, A. H. Moser, C. Grunfeld, and K. R. Feingold. 2000. Up-regulation of peroxisome proliferator-activated receptors (PPAR- $\alpha$ ) and PPAR-gamma messenger ribonucleic acid expression in the liver in murine obesity: troglitazone induces expression of PPAR-gamma-responsive adipose tissue-specific genes in the liver of obese diabetic mice. *Endocrinology*. **141**: 4021–4031.
15. Burant, C. F., S. Sreenan, K. Hirano, T. A. Tai, J. Lohmiller, J. Lukens, N. O. Davidson, S. Ross, and R. A. Graves. 1997. Troglitazone action is independent of adipose tissue. *J. Clin. Invest.* **100**: 2900–2908.
16. Daum, G. 1985. Lipids of mitochondria. *Biochim. Biophys. Acta*. **822**: 1–42.
17. Hoch, F. L. 1992. Cardiolipins and biomembrane function. *Biochim. Biophys. Acta*. **1113**: 71–133.
18. Hatch, G. M. 1994. Cardiolipin biosynthesis in the isolated heart. *Biochem. J.* **297**: 201–208.
19. Beleznai, Z., and V. Jancsik. 1989. Role of cardiolipin in the functioning of mitochondrial L-glycerol-3-phosphate dehydrogenase. *Biochem. Biophys. Res. Commun.* **159**: 132–139.
20. Fry, M., and D. E. Green. 1981. Cardiolipin requirement for electron transfer in complex I and III of the mitochondrial respiratory chain. *J. Biol. Chem.* **256**: 1874–1880.
21. Ohtsuka, T., M. Nishijima, K. Suzuki, and Y. Akamatsu. 1993. Mitochondrial dysfunction of a cultured Chinese hamster ovary cell mutant deficient in cardiolipin. *J. Biol. Chem.* **268**: 22914–22919.
22. Watkins, S. M., L. C. Carter, and J. B. German. 1998. Docosahexaenoic acid accumulates in cardiolipin and enhances HT-29 cell oxidant production. *J. Lipid Res.* **39**: 1583–1588.
23. Moore, S. A., E. Hurt, E. Yoder, H. Sprecher, and A. A. Spector. 1995. Reevaluation of the pathways for the biosynthesis of polyunsaturated fatty acids. *J. Lipid Res.* **36**: 2433–2443.
24. Sprecher, H., D. L. Luthria, B. S. Mohammed, and S. P. Baykousheva. 1995. *J. Lipid Res.* **36**: 2471–2477.
25. Voss, A., M. Reinhart, S. Sankarappa, and H. Sprecher. 1991. The metabolism of 7,10,13,16,19-docosapentaenoic acid to 4,7,10,13,16,19-docosahexaenoic acid in rat liver is independent of a 4-desaturase. *J. Biol. Chem.* **266**: 19995–20000.
26. Yang, B. C., T. G. Saldeen, J. L. Bryant, W. W. Nichols, and J. L. Mehta. 1993. Long-term dietary fish oil supplementation protects against ischemia-reperfusion-induced myocardial dysfunction in isolated rat hearts. *Am. Heart J.* **126**: 1287–1292.
27. Yang, B., T. G. Saldeen, W. W. Nichols, and J. L. Mehta. 1993. Dietary fish oil supplementation attenuates myocardial dysfunction and injury caused by global ischemia and reperfusion in isolated rat hearts. *J. Nutr.* **123**: 2067–2074.
28. Hock, C. E., L. D. Beck, R. C. Bodine, and D. K. Reibel. 1990. Influence of dietary n-3 fatty acids on myocardial ischemia and reperfusion. *Am. J. Physiol.* **259**: H1518–1526.
29. McLennan, P. L., T. M. Bridle, M. Y. Abeywardena, and J. S. Charnock. 1993. Comparative efficacy of n-3 and n-6 polyunsaturated fatty acids in modulating ventricular fibrillation threshold in marmoset monkeys. *Am. J. Clin. Nutr.* **58**: 666–669.
30. Pepe, S., and P. L. McLennan. 1996. Dietary fish oil confers direct antiarrhythmic properties on the myocardium of rats. *J. Nutr.* **126**: 34–42.
31. Leaf, A. 1995. Omega-3 fatty acids and prevention of ventricular fibrillation. *Prostaglandins Leukot. Essent. Fatty Acids*. **52**: 197–198.
32. Thai, T., C. Rodemer, A. Jauch, A. Hunziker, A. Moser, K. Gorgas, and W. Just. 2001. Impaired membrane traffic in defective ether lipid biosynthesis. *Hum. Mol. Genet.* **10**: 127–136.